doi:10.1093/plphys/kiab207 PLANT PHYSIOLOGY 2021: 186: 1908–1918

Plant Physiology®

Research Article

Herb and conifer roots show similar high sensitivity to water deficit

Ibrahim Bourbia [1], **Carola Pritzkow**[1] **and Timothy J. Brodribb** [1,*,†]

1 School of Natural Sciences, University of Tasmania, Hobart, TAS 7001, Australia

*Author for communication: timothy.brodribb@utas.edu.au
†Senior author.

I.B. and T.J.B. conceived and designed the experiment; I.B. and C.P. performed the experiment; I.B. analyzed the data and wrote the manuscript with revisions from T.J.B.
The author responsible for distribution of materials integral to the findings presented in this article in accordance with the policy described in the Instructions for Authors (https://academic.oup.com/plphys/pages/general-instructions) is: Name (timothy.brodribb@utas.edu.au).

Abstract

Root systems play a major role in supplying the canopy with water, enabling photosynthesis and growth. Yet, much of the dynamic response of root hydraulics and its influence on gas exchange during soil drying and recovery remains uncertain. We examined the decline and recovery of the whole root hydraulic conductance (*Kr*) and canopy diffusive conductance (g_c) during exposure to moderate water stress in two species with contrasting root systems: *Tanacetum cinerariifolium* (herbaceous Asteraceae) and *Callitris rhomboidea* (woody conifer). Optical dendrometers were used to record stem water potential at high temporal resolution and enabled non-invasive measurements of *Kr* calculated from the rapid relaxation kinetics of water potential in hydrating roots. We observed parallel declines in *Kr* and g_c to <20% of unstressed levels during the early stages of water stress in both species. The recovery of *Kr* after rewatering differed between species. *T. cinerariifolium* recovered quickly, with 60% of *Kr* recovered within 2 h, while *C. rhomboidea* was much slower to return to its original *Kr*. Recovery of g_c followed a similar trend to *Kr* in both species, with *C. rhomboidea* slower to recover. Our findings suggest that the pronounced sensitivity of *Kr* to drought is a common feature among different plant species, but recovery may vary depending on root type and water stress severity. *Kr* dynamics are proposed to modulate g_c response during and following drought.

Introduction

Efficient extraction of water by roots is essential for plant function, and a key determinant of growth and productivity in both natural and agricultural systems. Roots play a critical role in supplying the water lost as transpiration during the process of photosynthetic gas exchange, yet this function appears to be highly sensitive to even mild water stress (Kramer, 1950; Blizzard and Boyer, 1980; North and Nobel, 1991; Trifilò et al., 2004; Domec et al., 2006; Cuneo et al., 2016; Rodríguez- Domínguez and Brodribb, 2019; Cuneo et al., 2020). Recent work on olive (*Olea europaea* L.) suggests that declining root hydraulic conductance (*Kr*, here referred to as the flow pathway from the root surface to stem) under intensifying soil water deficit has a major impact on whole-plant hydraulic transport capacity, triggering stomatal closure (Rodríguez-Domínguez and Brodribb, 2019). Yet, it is unknown whether the root limitation of stomatal conductance during drought is a feature of diverse plant species, and if so how the dynamics of *Kr* recovery following rewatering after drought might influence gas exchange.

Xylem embolism has been widely accepted to be the main factor limiting hydraulic conductance of plant tissues

Received October 27, 2020. Accepted April 24, 2021. Advance access publication May 10, 2021

during acute episodes of drought (Tyree and Zimmermann, 2002; Brodribb and Cochard, 2009). However, at the root level, several studies have reported declines in *Kr* before xylem embolism. The declines in *Kr* have been most often attributed to a range of morphological, anatomical, and molecular changes, including cortical lacunae formation due to cellular dehydration and collapse (North and Nobel, 1991, 1992; Cuneo et al., 2016), suberization (Passioura, 1988; Cruz et al., 1992; North and Nobel, 1992; Gullo et al., 1998; Trifilò et al., 2004; Barrios-Masias et al., 2015; Brunner et al., 2015), and reduced aquaporin activity (Martre et al., 2001; North et al., 2004; Vandeleur et al., 2009; Maurel et al., 2015). The extent of the root responses mentioned above have been found to increase with increasing water stress severity, resulting in further loss in *Kr* (Carminati, 2013; Cuneo et al., 2016, 2020). This raises the likelihood that the severity of water stress may dictate the speed of root recovery responses following soil water replenishment (Kramer, 1950). For instance, roots subjected to severe stress might be expected to incur greater morphological and physiological adjustments, which would result in a greater delay in their functional recovery, thus a lag in reestablishment of plant gas exchange (Kramer, 1950). This has clearly been shown to be the case when plants have been subjected to acute water deficit sufficient to cause xylem cavitation (Brodribb et al., 2010; Rehschuh et al., 2020). However, it is unknown how *Kr*, when reduced by processes other than cavitation, is likely to recover when water returns.

Several studies suggest that the drought-induced decrease in *Kr* can be reversed when the soil is rewetted. But the speed and rate of this *Kr* recovery must be dependent upon the mechanism of its decline. In most cases, *Kr* recovery has been associated with the growth of new roots because most of the changes that occurred in the root system during drought were irreversible and permanently impeded radial flow of water within the root (e.g. cortical lacunae and suberin deposition ; Nobel and Sanderson, 1984; North and Nobel, 1991, 1996; Green and Clothier, 1995; Gullo et al., 1998; Cuneo et al., 2020). However, there is some evidence to suggest that *Kr* can be restored before root growth through renewed permeability of pre-existing roots (Nobel and Sanderson, 1984; North and Nobel, 1991). This might happen if the decline in *Kr* is mainly due to reversible collapse and shrinkage of root cortical cells. In this case, recovery may be achieved quickly by hydration and re-expansion of the cells, which can occur within minutes or hours as has been shown in leaves (Scoffoni et al., 2012; Zhang et al., 2016).

The kinetics of *Kr* recovery might also be species specific or related to the root system type. The root system of woody species consists mainly of old suberized or woody roots (~99% of the total root surface area; Kramer and Bullock, 1966) compared with roots of herbaceous species, which are composed mostly of highly permeable un-suberized thin roots (Boyer and Kramer, 1995; Gambetta et al., 2013; Ma et al., 2018). When subjected to drought, suberized roots can become permanently hydrophobic and may require longer time to regain permeability (Clarkson et al., 1987; North and Nobel, 1992; Cuneo et al., 2018). The suberized characteristic of woody roots combined with drought-induced changes in root biology may greatly slow the response of woody species' roots to soil rewatering following drought compared to herbaceous roots.

Until recently, methodological limitations made it difficult to measure *Kr* in situ in water-stressed plants. The few measurements of root water uptake during soil drying have been mainly performed on excised roots using methods such as the high-pressure flow meter, the root pressure probe, and the root-pressure chamber (Passioura, 1980; Frensch and Steudle, 1989; Hallgren et al., 1995; Tyree et al., 1995; Gullo et al., 1998). These methods are all destructive, therefore continuous monitoring of same individual (or root system) during water stress is not possible. Recently, Rodríguez-Domínguez and Brodribb (2019) introduced a rehydration method for measuring *Kr* in situ based on relaxation kinetics of stem water potential measured with a psychrometer. However, this instrument has various drawbacks, including the installation on soft herbaceous plants, the temporal limitation of a 10-min window between measurements, low accuracy at high stem water potential (higher than −0.5 MPa) and the low degree of stability under fluctuating temperatures, making it unsuitable for quick rehydration measurements.

In this study, we introduce a nondestructive method for measuring *Kr* during water stress. This technique is based on examining the relaxation kinetics of the water potential (using tissue width variation as a water potential proxy) in rehydrating intact roots monitored at high temporal resolution (<20 s) using an "optical dendrometer."

Using this technique, we measured the decline and recovery of *Kr*, as well as canopy diffusive conductance (g_c) during drought and rewatering cycles in two species with distinct ecological features and root systems: *Tanacetum cinerariifolium* (perennial herb) with herbaceous roots and *Callitris rhomboidea* (hardy conifer) with woody roots. Post-drought recovery kinetics of *Kr* were monitored immediately after rewatering as a means of understanding the mechanisms of *Kr* decline whether they are related to permanent or reversible changes in the root system. We hypothesized that, in both species, *Kr* would show a similar high sensitivity to soil water deficit, and that g_c would be limited by *Kr* both during drying and recovery. The herbaceous *T. cinerariifolium* was predicted to recover *Kr* faster upon rewatering than the woody *C. rhomboidea*, with the extent and speed of this recovery affected by the magnitude of the drought imposed.

Results

Response of *Kr* and g_c to water stress

Kr was similarly highly sensitive to mild soil water deficit, with depressions occurring after soil water potential (Ψ_{soil}) fell below −1 MPa in both studied species (Figure 1). *Kr* decreased by ~80% in the range −1.5 to −2 MPa compared

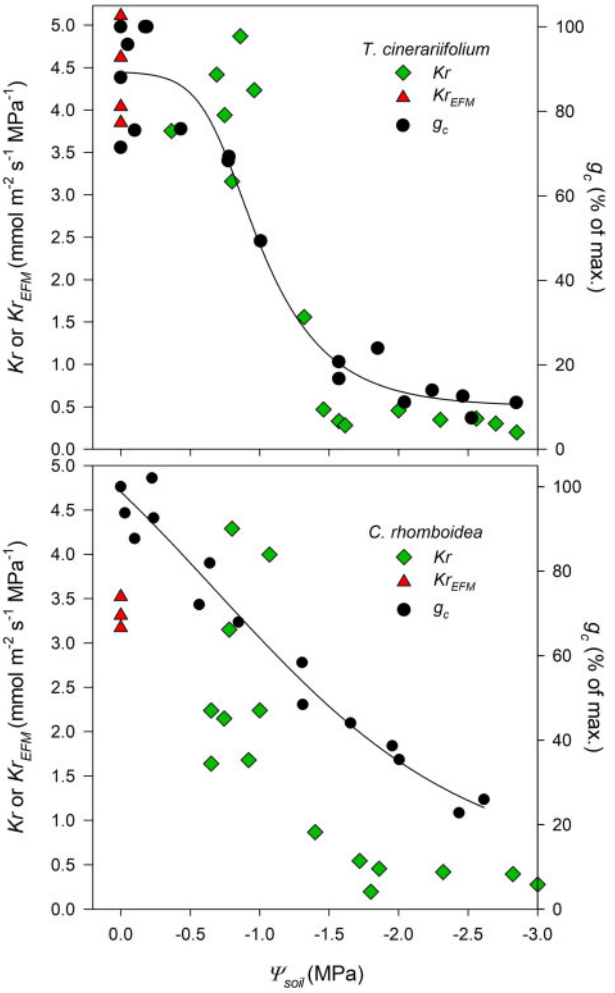

Figure 1 Response of *Kr* and g_c to water stress. The response of *Kr* (measured using the Ψ_{stem} relaxation kinetics resulted from rehydrating intact plants through the soil (green diamonds; $n = 6–7$ plants)), and g_c (black circles; $n = 3$ plants) to increasingly negative Ψ_{soil} in the herbaceous *T. cinerariifolium* and the woody *C. rhomboidea*. Red triangles (Kr_{EFM}) correspond to *Kr* values measured using the EFM in well-watered plants at midday (12:00–14:00) during steady-state conditions. The solid black line is a four-parameter sigmoidal regression fitted to the pooled midday g_c versus Ψ_{soil} data for both species.

with that measured at minimum water stress in both species (Figure 1).

Kr measured at minimum Ψ_{soil} represented a plateau in both species, thus it was considered as maximum *Kr* (*Kr*-max). Mean *Kr*-max was significantly higher in the herbaceous *T. cinerariifolium* (4.06 ± 0.22 mmol m^{-2} s^{-1} MPa^{-1}) compared with the woody *C. rhomboidea* (2.74 ± 0.37 mmol m^{-2} s^{-1} MPa^{-1}; $P < 0.05$; Figure 1). Furthermore, the mean *Kr*-max measured at minimum Ψ_{soil} with the rehydration method was similar to Kr_{EFM} determined with the evaporative flux method (EFM) in unstressed well-watered plants (4.4 ± 0.24 and 3.33 ± 0.08 mmol m^{-2} s^{-1} MPa^{-1} in the herbaceous *T. cinerariifolium* and the woody *C. rhomboidea*, respectively; Figure 1).

In both species, declines in g_c occurred early during drying and over the same range of Ψ_{soil} as *Kr* (Figure 1). However, despite similar *Kr* sensitivity to Ψ_{soil}, in the herbaceous *T. cinerariifolium* g_c fell from 80% to 20% of maximum within a narrow range of Ψ_{soil} (between −0.85 and −1.5 MPa), displaying a steeper reduction in midday g_c during drying compared with the woody *C. rhomboidea*, which closed stomata more slowly with 20% closure occurring at $\Psi_{soil} < -2.5$ MPa (Figure 1). The modeled g_c ($g_{c\text{-mod}}$) using the experimentally measured *Kr* during increasing soil water stress were generally in good agreement with the measured g_c values (Supplemental Figure S5). However, in the woody *C. rhomboidea*, g_c was 50% higher than predicted by the model at mild water stress despite the drop in *Kr*.

Short-term recovery of Kr from mild and moderate water stress

The two studied species varied substantially in their dynamic response of *Kr* to rewatering after water stress. In the herbaceous *T. cinerariifolium*, the rate and kinetics of *Kr* recovery were dependent on the extent of drought severity imposed. *Kr* of plants exposed to mild stress responded quickly to rewatering, recovering 60.89 ± 7.91% of its pre-drought value (*Kr*-max) within 2 h of rewatering (i.e. 45.41% increase in *Kr*; Figure 2), whereas plants subjected to moderate stress returned to only 16.68 ± 3.54% of *Kr*-max during this first 2-h period (Figure 2). In contrast, *Kr* of the woody *C. rhomboidea* did not respond to rewetting within the 2-h observation period, remaining at around 15%–20% of *Kr*-max regardless of the severity of the drought treatment (Figure 2).

Long-term recovery of *Kr* from moderate water stress and coordination with g_c recovery

Further monitoring over 64 h following rewatering of plants dried close to stomatal closure (i.e. moderate stress of approximately −2.5 MPa; Ψ_{soil}) confirmed a faster recovery of Kr_{EFM} measured with EFM in the herbaceous *T. cinerariifolium* than the woody *C. rhomboidea*. Fifteen hours after rewatering, in the herbaceous *T. cinerariifolium*, Kr_{EFM} had recovered to a mean of 50.78 ± 5.28% of maximum Kr_{EFM} and increased further to 75.78 ± 5.22% after 64 h (Figure 3). In contrast, Kr_{EFM} showed a low recovery rate 15 h after rewatering in woody *C. rhomboidea* (19.56 ± 1.46% of pre-drought value), increasing to only ~67.69 ± 5.83% of maximum Kr_{EFM} after 64 h (Figure 3).

The herbaceous *T. cinerariifolium* plants rehydrated rapidly such that Ψ_{stem} recovered to control levels within 15 h after rewatering, while the woody *C. rhomboidea* plants required 40 h for midday Ψ_{stem} to recover (Figure 4). Compared with the quick recovery of midday Ψ_{stem}, some hysteresis of g_c (midday g_c) recovery was observed after re-watering in both species. g_c recovery followed a similar pattern to that of Kr_{EFM}, especially in the herbaceous *T. cinerariifolium*, but was slightly faster than Kr_{EFM} recovery in the woody *C. rhomboidea* (Figure 3). In both species, g_c showed a partial recovery 15 h after rewatering, returning to 48.16 ± 5.72% and

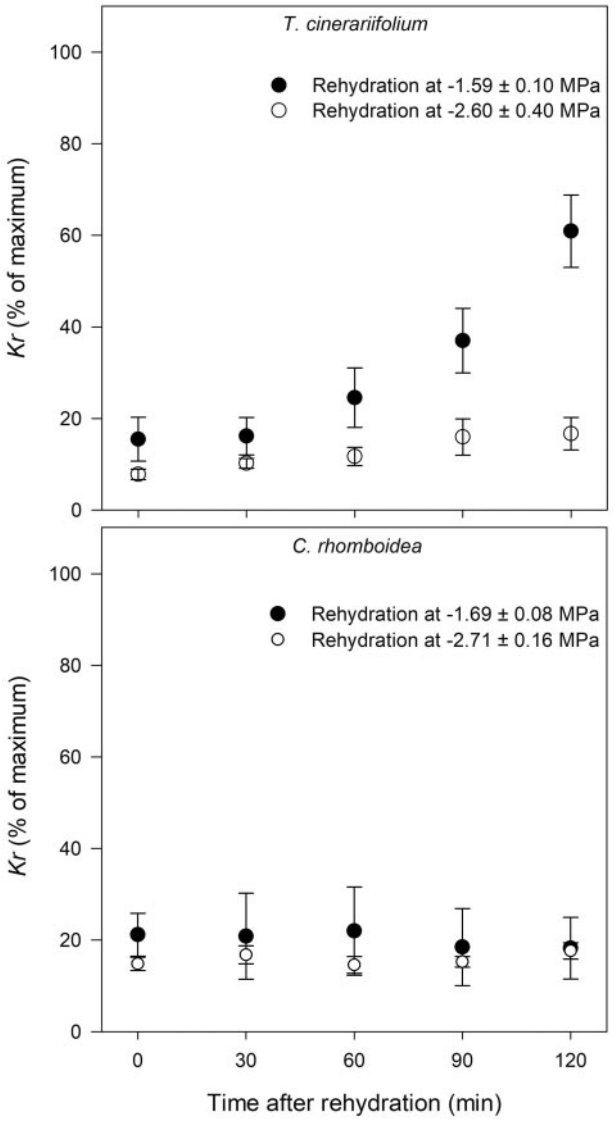

Figure 2 Recovery kinetics of *Kr* immediately after rewatering from mild and moderate water stress. Responses of *Kr* of the herbaceous *T. cinerariifolium* ($n = 4–5$) and the woody *C. rhomboidea* ($n = 3–4$) to rewetting from two levels: mild (Ψ_{soil} approximately −1.5 MPa) and moderate soil water stress (Ψ_{soil} approximately −2.5 MPa). Values are means ± SE expressed as a percentage of *Kr*-max measured in each plant at minimum water stress ($\Psi_{soil} \geq$ -1 MPa).

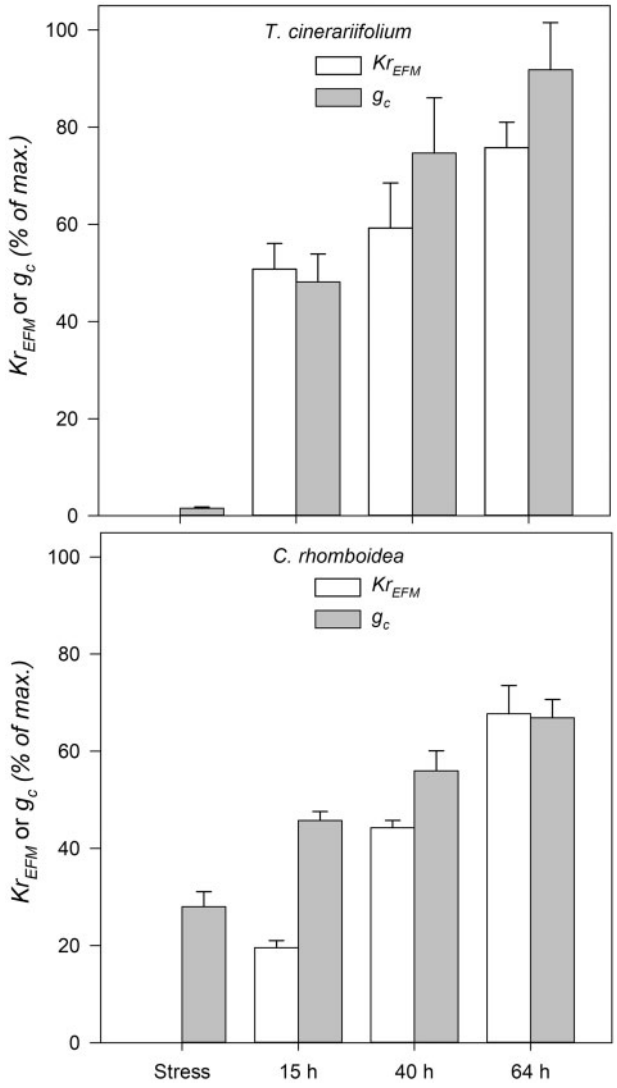

Figure 3 Recovery of *Kr* measured using the EFM (Kr_{EFM}) and g_c from moderate water stress. Time-course of recovery of Kr_{EFM} measured using the EFM at midday (12:00–14:00 h) during steady-state conditions and g_c after rewatering from moderate soil water deficit Ψ_{soil} of approximately −2.5 MPa. Values are means ± SE ($n = 3$ plants) expressed as a percentage of pre-drought maximum Kr_{EFM} measured in each plant of both species.

45.73 ± 1.84% of g_c-max (measured in well-watered conditions) in the herbaceous *T. cinerariifolium* and the woody *C. rhomboidea*, respectively (Figure 3). Over the subsequent days, g_c recovery remained slower and incomplete in the woody *C. rhomboidea* (66.88 ± 3.73% of g_c-max after 64 h), while it returned close to pre-drought values (91.81 ± 9.74% of g_c-max) in the herbaceous *T. cinerariifolium* after 64 h of recovery (Figure 3).

Discussion

The dynamics of *Kr* were measured by rehydration kinetics using an optical dendrometer to track rapid changes in water potential, thus allowing measurements of *Kr* in intact root systems under decreasing Ψ_{soil} without the need of excising or extracting them from soil. Our results demonstrate that although the decline of *Kr* during dehydration is similar in two functionally disparate species, the recovery of *Kr* is distinct, thereby differentiating the recovery of gas exchange.

Convergent responses of *Kr* to water stress

By monitoring the kinetics of plant rehydration after rewatering from different water stress levels, we were able to detect a similar sharp decline in *Kr* during early stages of water stress in the two distinctly different species studied here. Similar patterns have been observed in the few previously measured species, such as olive (Gullo et al., 1998; Rodriguez-Dominguez and Brodribb, 2019), grapevine

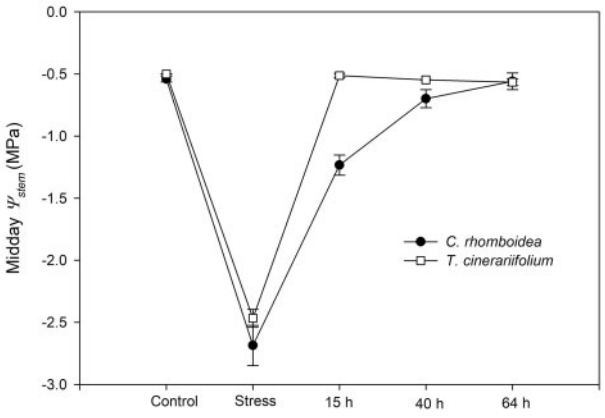

Figure 4 Recovery of midday stem water potential (Ψ_{stem}) from moderate water stress. Midday stem water potential (Ψ_{stem}) before and following rewatering after exposing plants to moderate soil water stress $\Psi_{soil} \sim -2.5$ MPa corresponding to >85% and 75% stomatal closure in the herbaceous *T. cinerariifolium* and the woody *C. rhomboidea*, respectively. Values are mean ± SE ($n = 3$ plants).

(Cuneo et al., 2016), soybean (Blizzard and Boyer, 1980), and desert succulents (North and Nobel, 1991, 1992, 1996), confirming a high sensitivity of *Kr* to soil water deficit. The similar high sensitivity of *Kr* to water stress observed in these species is impressive considering the stark functional and phylogenetic contrasts between these species.

Xylem cavitation is an unlikely explanation for the patterns observed here because 80% of the reduction in *Kr* occurred as Ψ_{soil} declined to −1.5 MPa (Figure 1), which is much higher (less negative) than the Ψ required to trigger xylem cavitation in either of these highly cavitation resistant species (Brodribb et al., 2010; Bourbia et al., 2020). The *Kr* declines we observed during early soil drying may be due to changes in root morpho-anatomical properties such as cortical lacunae formation, deposition of suberin, and root shrinkage (Passioura, 1988; North and Nobel, 1991, 1992; Nobel and Cui, 1992; Gullo et al., 1998; Cuneo et al., 2016).

g_c dynamics during water stress may be driven by drought-induced *Kr* limitation

Kr declined in parallel with stomatal closure in both species (Figure 1), suggesting a limitation of stomatal opening by reduced *Kr* during drought. The concurrent decline in *Kr* and gas exchange observed in the two species studied here is similar to that reported in soybean (Blizzard and Boyer, 1980) and olive (Rodríguez-Domínguez and Brodribb, 2019), despite clear ecological, anatomical, and functional differences between these species. This suggests that the correspondence between root hydraulic limitation and stomatal closure during drought may be a general feature across species. In some species, stomatal closure has been proposed to be driven by a drop in the above-ground hydraulic conductance (e.g. leaf) that reportedly occurs before xylem embolism (Holloway-Phillips and Brodribb, 2011; Scoffoni et al., 2018; Wang et al., 2018). However, in the two species studied here, declines in leaf hydraulic conductance were not observed within the range of water potential where substantial drops in *Kr* occurred (Brodribb and Cochard, 2009; Bourbia et al., 2020). This was also evidenced here by the faster relaxation of excised compared with intact petioles/branchlets after rehydration from moderate stress (approximately −2.5 MPa; Supplemental Figure S4). The slow relaxation observed here in intact petioles/branchlets is caused by reduced water uptake by root due to low *Kr* induced by moderate water stress.

Conflicting results have been reported in the literature regarding the limiting hydraulic conductance in the soil–plant system constraining water flow, thus gas exchange during soil drying. Some theoretical and experimental studies have argued that *Kr* becomes the limiting hydraulic conductance in the soil–plant system during soil drying (Andrews and Newman, 1969; Newman, 1969; Hansen, 1974; Blizzard and Boyer, 1980). However, others have argued that K_{soil} decreases by several orders of magnitude compared with *Kr* even under mild water stress (Gardner and Ehlig, 1962; Passioura, 1980; Hainsworth and Aylmore, 1986). Our results suggest that the decline in gas exchange during soil drying is likely driven by *Kr* limitation as the magnitude of the decline in *Kr* observed at mild and moderate stress were sufficient to prevent maximum stomatal opening, especially in the herbaceous *T. cinerariifolium* (according to a hydraulic model; Supplemental Figure S5). However, the woody *C. rhomboidea* maintained a higher than expected g_c at mild water stress despite the decrease in *Kr*, and this may be due to a significant dependence on capacitance for water supply in this species (Scholz et al., 2011).

A recent modeling work by (Carminati and Javaux, 2020) has also suggested that K_{soil} is the main constraint on water flow in soil–plant system. Interestingly, the range of K_{soil} decline predicted by these models matches quite closely our observed behavior of *Kr* under drought, suggesting that the hydraulic connection between water in the soil and water in the xylem declines in parallel as soils dehydrate in both species. Therefore, we suggest that the decrease in *Kr* and K_{soil} could both contribute to the decline of g_c during drying, but further work is needed to disentangle the relative contributions of these hydraulic parameters on the dynamics of g_c, particularly under mild drought stress. However, after rewatering following drought stress, the loss in K_{soil} can be quickly reversed (within seconds when soil is submerged), whereas the loss in *Kr* may require several days to recover, thus becoming the predominant factor influencing leaf water potential and limiting full stomatal reopening.

Kr recovery kinetics is species and water stress intensity dependent

Upon rewatering, the two species studied here displayed different recovery kinetics in *Kr* depending on the level of drought stress imposed, with the herbaceous *T. cinerariifolium* being quick to recover. The distinctly different recovery kinetics in *Kr* suggests that different mechanisms may be responsible for *Kr* depression in the two studied species.

The extent of root hydraulic recovery measured immediately after rewatering (within 2 h of rewatering; Figure 2) may provide some clues as to what causes the initial dramatic decline in *Kr* during early water stress stages. The quick recovery of *Kr* observed in the mildly drought-stressed plants of the herbaceous species *T. cinerariifolium* (i.e. 60% within 2 h of rewatering) implies that the decline in *Kr* in the beginning of drought was more likely induced by transient (rapidly reversible) modifications in the root system, such as shrinkage and collapse of undamaged cortical cells. Further, this quick recovery eliminates the possibility that it was achieved by root growth as suggested by previous studies linking *Kr* recovery to new root growth (Kramer, 1950; Nobel and Sanderson, 1984; North and Nobel, 1991, 1996; Green and Clothier, 1995; Dubrovsky et al., 1998; Gullo et al., 1998; Cuneo et al., 2020). Rapid recovery of *Kr* without corresponding root growth upon mild drought has also been observed in roots of the desert succulent *Agave deserti* and was associated with renewed permeability of existing roots through hydration and re-expansion of their collapsed cortical cells (North and Nobel, 1991). In contrast, the lack of *Kr* recovery in mildly drought-stressed plants of the woody species *C. rhomboidea* immediately after rewatering suggests that the root system, particularly fine roots, incurred significant irreversible changes such as suberization and formation of cortical lacunae. In this case, growth of new laterals or regrowth from the distal meristem would be needed to recover maximum root water uptake in this species (North and Nobel, 1991, 1996; Gullo et al., 1998; Cuneo et al., 2020).

Further monitoring of *Kr* recovery over 64 h of rewatering measured with the EFM (Kr_{EFM}) in plants exposed to moderate water stress (approximately −2.5 MPa) also confirmed a slower recovery of *Kr* in the woody species *C. rhomboidea* compared to the herbaceous species *T. cinerariifolium*. The difference in *Kr* recovery kinetics may be associated with the contrasting ecology of herbaceous and woody species. Compared to woody species, most herbaceous species have shallow root systems and are often exposed to soil water deficit from the combined effects of competition and rapid soil evaporation (Schenk and Jackson, 2002; Rossatto et al., 2014). Establishment success of these species under such conditions should greatly depend on their ability to readily resume root function and exploit newly available soil moisture.

Full stomatal reopening was inhibited following post-stress rewatering despite the recovery of midday Ψ_{stem} to pre-drought levels in both species (Figures 3 and 4). Similar patterns of incomplete stomatal conductance recovery after drought-induced stomatal closure have been reported in some species where drought stress was not associated with irreversible xylem cavitation (Liang and Zhang, 1999; Loewenstein and Pallardy, 2002; Pou et al., 2008; Yan et al., 2017), but the processes underlying this delay are not well understood. Residual ABA has been suggested as a possible cause of the observed delay in stomatal conductance recovery after rewatering (Brodribb and McAdam, 2013). However, in many species, xylem sap or leaf apoplast ABA has been reported to quickly return to control levels (1 d after rewatering) and before complete recovery of stomatal conductance after moderate drought (Correia and Pereira, 1995; Liang et al., 1997; Liang and Zhang, 1999; Pou et al., 2008; Torres-Ruiz et al., 2015; Ruehr et al., 2019), suggesting that additional factors may also contribute to the dynamics of gas exchange recovery. If stomatal reopening is delayed by residual ABA rather than compromised hydraulic function, then midday Ψ_{stem} in post-drought plants should be higher (less negative) than that in pre-drought plants because of the low g_c (Brodribb and Cochard, 2009). However, in our study, differences in midday Ψ_{stem} after rewatering and before drought were negligible in both species (after 40 h of rewatering in the woody *C. rhomboidea*; Figure 4), despite the low g_c measured in rewatered plants (Figure 3). This suggests that the low recovery of g_c in rewatered plants was mainly constrained by water supply due to low *Kr* induced by moderate drought stress. This is further supported by the similar recovery trend of *Kr* and g_c after rewatering in both species. Furthermore, the technique of soil rewetting used here (soil flooding) should quickly restore K_{soil}, meaning that the slow recovery of g_c observed here following drought is primarily due to low *Kr* as opposed to low K_{soil}.

Conclusion

Overall, our findings highlight the importance of *Kr* dynamics during changes in soil water deficit. The demonstration that the roots of different species are similarly susceptible to dramatic reductions in hydraulic conductance during mild and moderate water deficit has major implications for predicting plant behavior during dynamic water stress. Such large changes in *Kr* may dominate the total flow pathway in the plant, thus determining rates of photosynthetic decline and recovery as well as the susceptibility to irreversible damage by cavitation (Brodribb et al., 2020). Further work is necessary to elucidate the causes behind such dynamic root behavior and its influence on plant gas exchange in diverse plant species growing in different soil types and conditions. This work will be greatly facilitated by the method presented here for measuring *Kr* in intact whole root systems.

Materials and methods

Plant material and glasshouse conditions

We grew individuals of pyrethrum (*T. cinerariifolium* (Trevir.) Sch. Bip.) and *C. rhomboidea* R. Br. ex A. Rich. & Rich. seedlings in glasshouse facilities at the University of Tasmania. Plants of the herbaceous *T. cinerariifolium* were 2-years old and were obtained from a commercial growing site in northern Tasmania. The woody *C. rhomboidea* seedlings ranged from 80 to 100 cm in height. Plants were potted in 5-L (*T. cinerariifolium*) and 2-L (*C. rhomboidea*) pots using potting mix (medium 7:4 mix of composted fine pine bark and coarse washed river sand). This potting mix was chosen to facilitate a rapid rewetting of the root system upon rewatering. Plants were grown under unfiltered natural light in a

controlled glasshouse cell (day/night temperature 25°C/15°C, day/night relative humidity 40%/80%) equipped with industrial circulation fans providing constant air movement.

Temperature and relative humidity in the glasshouse cell remained constant throughout the experiment and were monitored with an HMP45AC temperature/humidity probe (HMP45AC; Vaisala Inc., Helsinki, Finland) placed close to the measured plants, and logged on a CR850 datalogger (Campbell Scientific, Logan, UT, USA).

Rehydration kinetics and *Kr* response to water stress

In both species, the impact of water stress on *Kr* (mmol s^{-1} m^{-2} MPa^{-1}) was measured under nonsteady-state conditions by examining the kinetics of stem water potential (Ψ_{stem}) relaxation (or water flow) during the rehydration of intact plants dehydrated to different levels of water stress (Rodriguez-Dominguez and Brodribb, 2019). Unlike previous application of this method, Ψ_{stem} relaxation was measured at high temporal resolution using petiole/branchlet width (as a water potential proxy) measured with an optical dendrometer (see below). *Kr* was determined by assuming the rehydrating plant behaved as a capacitor discharging (water potential rising to zero) through a resistor (Brodribb and Holbrook, 2003) and using Equation (1) by fitting an exponential curve through the first 15 min (5–15 datapoints; see Supplemental Figure S1) of Ψ_{stem} relaxation data following rewatering:

$$\Psi_f = \Psi_0 \times e^{Kr \times t / C_{plant}} \quad (1)$$

where Ψ_o is the initial Ψ_{stem} before rehydration (MPa), Ψ_f is the final Ψ_{stem} (MPa) after rehydration for t seconds, and C_{plant} is whole plant capacitance (mmol m^{-2} MPa^{-1}).

Kr was determined in six to seven plants per species at three different levels of soil water stress (Ψ_{soil}). Water stress levels were determined from previous experiments showing sharp declines in *Kr* at Ψ_{stem} lower than −1 MPa (i.e. in olive [*O. europaea* L.]; Rodriguez-Dominguez and Brodribb, 2019). These water deficits were created by withholding watering for different periods of time while monitoring Ψ_{stem} using optical dendrometer based on the strong correlation between petiole/branchlet width and Ψ_{stem} (see the section below; "Optical dendrometer"): minimum stress ($-0.36 \geq \Psi_{soil} \geq -1$ MPa), mild stress ($-1.3 \geq \Psi_{soil} \geq -1.8$ MPa) and moderate stress or approximate stomatal closure ($-2 \geq \Psi_{soil} \geq -3$ MPa). Plants were first subjected to minimum water stress then rehydrated, then exposed to mild water stress and rehydrated again, then given sufficient time to recover (1 week) before subjecting them to moderate water stress. After reaching the desired water stress level and before rewatering, plants were covered with a wet plastic bag and placed in the dark for at least 2–3 h to ensure stomatal closure and allow Ψ_{stem} and Ψ_{soil} to come to equilibrium. Therefore, Ψ_{soil} was assumed to be equivalent to Ψ_{stem} before rewatering (after equilibration in the dark). Ψ_{stem} before rewatering was verified using a leaf measured with a Scholander chamber (PMS, Albany, OR, USA). The root rehydration kinetics method requires water to be immediately in contact with roots, so plants were rewatered rapidly by submerging pots in a bucket filled with sufficient water to cover the pots. Pots were kept submerged for at least 1 h.

Kr values were standardized to the viscosity of water at 20°C (Korson et al., 1969) and plotted against Ψ_{soil}, which was assumed to be equivalent to Ψ_{stem} measured before rewatering.

Optical dendrometer

High temporal resolution of water potential was necessary to compute *Kr* from rehydration. This could not be provided with standard methods; hence we designed an optical dendrometer that allowed petiole and branchlet width to be continuously monitored and used as a precise proxy for xylem water potential.

Changes in the width of petioles in the herbaceous *T. cinerariifolium* or determinate branchlets (<3 mm in diameter) in the woody *C. rhomboidea* were used as a proxy for water potential dynamics in the stem xylem (assuming a negligible pressure gradient exists between the petiole and the root collar). Calibration of the relationship between predawn petiole/branchlet width and predawn Ψ_{stem} was undertaken by simultaneous and continuous measurements of width and Ψ_{stem}. Petiole/branchlet widths were monitored on the same plants targeted for *Kr* measurements during the drying-rewatering experiment using an optical dendrometer (MiCAM). Petioles and branchlets were clamped securely in MiCAM; a custom-built OpenSourceOV (http://www.opensourceov.org) 3D-printed clamp fitted with a Hastings triplet achromatic lens (approximately ×30 magnification), a small eight mega-pixel Raspberry Pi camera, and white light-emitting diodes. The clamp assembly was connected to a Raspberry Pi microcomputer (Raspberry Pi Foundation, Cambridge, UK, http://www.raspberrypi.org) programmed to acquire images at regular intervals (e.g. 1–3 min; Supplemental Figure S2). During image acquisition, the captured petioles/branchlets were backlit, and the camera shutter-speed was set sufficiently low (i.e. limiting the number of photons registered by the camera light sensors) such that the petioles/branchlets in the foreground are in shadow and predominantly composed of dark pixels. The dark captured petiole/branchlet images in the foreground were then automatically extracted from the lighter background using the Otsu thresholding method (Otsu, 1979), and the number of dark foreground pixels (i.e. petiole/branchlet) was automatically counted to provide petiole/branchlet width.

Ψ_{stem} measurements were performed with stem psychrometers (PSY1; ICT International, Armidale, NSW, Australia) installed on the flowering stem for the herbaceous *T. cinerariifolium* and the main stem for the woody *C. rhomboidea* plants (Supplemental Figure S2). Predawn Ψ_{stem} measurements were also performed periodically on leaves once the soil began to dry down using a Scholander pressure chamber to validate the plant water status.

Petiole/branchlet width and Ψ_{stem} measured with the psychrometer were tightly linearly correlated ($r^2 = 0.99$, $P < 0.001$) during slow drying (between 0 and −3 MPa; Ψ_{soil}) and fast rehydration after rewatering (Figure 5, inset). Ψ_{stem} relaxation monitored with the optical dendrometers (based on the tight correlation between Ψ_{stem} petiole/branchlet width) during rehydration was used to calculate *Kr* (Equation (1)) after rewatering from different levels of water stress.

Whole plant capacitance

The calculation of *Kr*, as described in Equation (1), requires the knowledge of whole plant capacitance (C_{plant}). C_{plant} was obtained for each plant used for *Kr* measurements by simultaneously measuring water potential and whole plant mass during a dry-down from 0 to −3 MPa. At the end of drying/rehydration experiment, plants were removed from the pots and their roots were gently rinsed to remove all soil. A stem psychrometer was attached to the flowering stem for the herbaceous *T. cinerariifolium* and stem for woody *C. rhomboidea* to monitor Ψ_{stem} during drying. The roots were carefully dried with absorbent paper, then plants were placed onto a balance (PG5002-S, 5100 9 0.01 g; Mettler-Toledo, GmbH, Greifensee, Switzerland) and their mass (g) and Ψ_{stem} (MPa) was recorded at 10-min interval during drying. Plants were allowed to dry slowly in the dark until their Ψ_{stem} reached −3 MPa (~2 d). C_{plant} was determined from the slope of the linear relationship between Ψ_{stem} and mass measured throughout drying and normalized by total plant projected leaf area (m^2) (Supplemental Figure S3).

We treated each plant as a single capacitor fed through the root resistor for two reasons:

(1) The bulk of resistance was found to be upstream of different plant capacitors (i.e. in the root system) in both species as shown by the faster relaxation of excised compared with intact petioles/branchlets, regardless of water stress severity (e.g. rehydration from Ψ_{stem} ~ −2.5 MPa; Supplemental Figure S4). Therefore, the potential gradient from root to mesophyll was assumed to be uniform during rehydration.

(2) In both species, stem and leaf (including petiole) hydraulic conductance has been reported to be constant in the range of Ψ_{soil} where *Kr* was measured (Brodribb et al., 2010; Bourbia et al., 2020). This suggests that the different capacitors in the plant would remain hydraulically well connected (during drying and rehydration), thus rehydrate following the same dynamic after rewatering. This was clearly evidenced by the concurrent change in Ψ_{stem} measured with the psychrometer at the stem level and petiole/branchlet width during slow drying and fast increase in water potential following rewatering in both species (Figure 5).

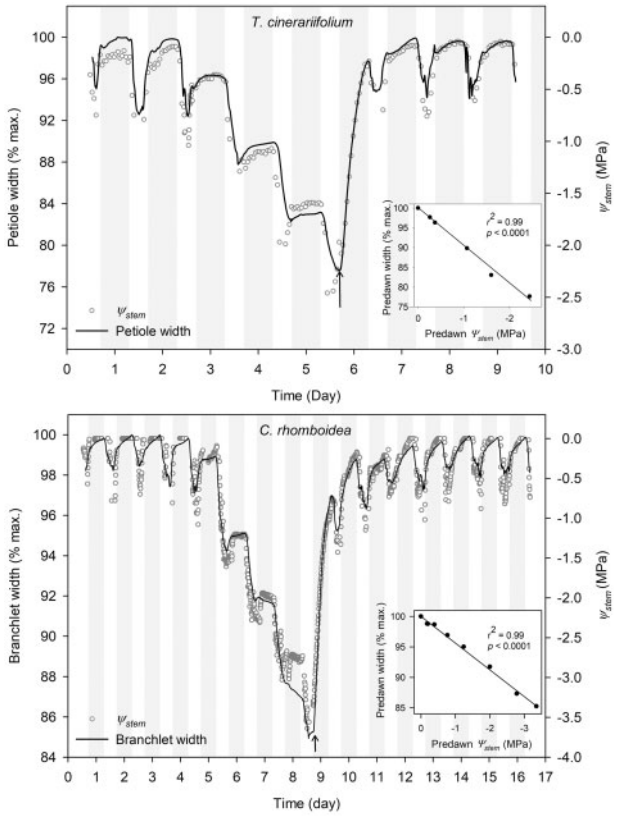

Figure 5 Diurnal variations of petiole and branchlet width recorded by optical dendrometers, and stem water potential Ψ_{stem} measured with a stem psychrometer. Diurnal variations of tissue width recorded by optical dendrometers in the herbaceous *T. cinerariifolium* (petiole) and the woody *C. rhomboidea* (branchlet; black solid line) calculated as a ratio of petiole/branchlet width : maximum width (measured at pre-dawn in well-hydrated conditions), and stem water potential Ψ_{stem} (gray open circles) measured with a stem psychrometer in well-watered conditions and during drought. Relationship between predawn Ψ_{stem} and predawn tissue width (inset). A linear regression was used to quantify the correlation between predawn width and predawn Ψ_{stem} (inset). The two plants presented here are separate from those used for *Kr* calculations. Vertical gray bars represent night periods and arrow indicates rewatering.

Validation of *Kr* using the EFM in well-watered plants

The root rehydration technique used in this study was not suited for measuring *Kr* in well-watered plants (with soils at field capacity), thus it was uncertain whether *Kr* measured with the rehydration technique at minimum water stress represented *Kr*-max or if it was higher in unstressed well-watered plants. Therefore, *Kr* in unstressed well-watered plants was measured in three plants per species using the EFM (Tsuda and Tyree, 2000) during steady-state conditions as described in Equation (2). This *Kr*, hereafter referred to as Kr_{EFM} (mmol s^{-1} m^{-2} MPa^{-1}), was calculated as follow:

$$Kr_{EFM} = \frac{E}{\Psi_{soil} - \Psi_{stem}} \quad (2)$$

Where *E* is midday canopy transpiration rate (mmol m^{-2} s^{-1}), Ψ_{stem} was measured with a pressure chamber on non-evaporating leaves (enclosed in plastic bags covered with aluminum foil for at least 2 h to ensure equilibration

between leaf and stem water potential), and Ψ_{soil} was assumed to be close to 0 MPa because soils were watered to field capacity before measurements.

E was measured gravimetrically in each plant with a balance (XS6002S; Mettler-Toledo GmbH, Greifensee, Switzerland) at midday between 1,200 and 1,400 h (during which time transpiration and Ψ_{stem} were at steady state in both species). *E* was then normalized by the projected whole-plant leaf area measured at the end of the experiment.

Response of g_c to water stress

g_c response to water stress was measured in three potted plants of each species to investigate whether stomata behave similarly to *Kr* during increasing water stress. Plants were maintained under the standard glasshouse conditions and remained unwatered while the pots were bagged and covered in foil during monitoring over 5–7 d. During this time, the soils dried sufficiently for stomata to become mostly closed, thus allowing the relationship between Ψ_{soil} and g_c to be determined.

Daily g_c during drying was calculated from time-averaged *E* measured gravimetrically in each plant at midday divided by the mole fraction vapor pressure deficit (VPD; Jarvis and McNaughton, 1986). Daily Ψ_{stem} during drying was measured in each plant every 20 min using a stem psychrometer attached to flowering stems for the herbaceous *T. cinerariifolium* and the main stem of the plant at ~20–30 cm from the base for the woody *C. rhomboidea*.

Similar to *Kr*, g_c was plotted against midday Ψ_{soil} that was assumed to be halfway between predawn Ψ_{stem} the day of measurement and the day after measurement. In each plant, g_c was expressed as a percentage of mean maximum g_c measured at the start of the dry-down experiment when plants were well hydrated.

Short-term recovery of *Kr* immediately after rewatering from mild and moderate water stress

We determined how *Kr* changed during the first 2 h following rewatering in plants exposed to mild and moderate water stress. This allowed differentiation between rapidly recoverable *Kr* from slower root system recovery processes occurring over the days following rewatering (see below "long-term recovery of *Kr* and g_c after rewatering from moderate water stress"). For each plant, short-term trajectory of *Kr* recovery was calculated the same way as the initial *Kr* measured at rewatering every 30 min during the first 2 h of rehydration (Supplemental Figure S1). *Kr* recovery from mild and moderate water stress of each plant was expressed as a percentage of *Kr*-max measured in the same plant at minimum water stress. *Kr*-max is defined here as the *Kr* measured at minimum soil water deficit.

Long-term recovery of *Kr* and g_c after rewatering from moderate water stress

Long-term *Kr* recovery (Kr_{EFM}) after rewatering following moderate Ψ_{soil} was determined using the EFM (Equation (2)). We also investigated how the recovery of g_c following rewatering after moderate drought was related to the recovery of Kr_{EFM}. Initially, g_c and Kr_{EFM} were measured over 3 d in three unstressed well-watered individuals per species, and the values were used to represent the maximum pre-drought levels of each parameter for each individual. These plants were then dried down to moderate water stress (Ψ_{soil} approximately −2.5 MPa), a target water potential associated with 85% and 75% stomatal closure in the herbaceous *T. cinerariifolium* and the woody *C. rhomboidea*, respectively, and >80% reduction in *Kr* in both species (based on measured g_c and *Kr* data). When the soil reached the targeted Ψ_{soil} (approximately −2.5 MPa), plants were re-watered and daily watering was resumed. Kr_{EFM} and g_c were then measured at midday over a period of 3 d after rewatering (at 15, 40, and 64 h after rewatering). Kr_{EFM} and g_c during recovery were expressed as a percentage of maximum pre-drought values (measured before drought in unstressed well-watered plants).

Modeling the impact of *Kr* dynamics on midday g_c

We assessed the effect of observed *Kr* dynamics measured with an independent rehydration technique on modeled g_c ($g_{c\text{-mod}}$) at the three levels of water stress (Ψ_{soil} approximately −0.5, −1.5, and −2.5 MPa) at which *Kr* was measured using the following hydraulic model:

$$g_{c-mod} = \frac{Kr \times (\Psi_{soil,md} - \Psi_{stem,md})}{VPD} \quad (3)$$

Where $g_{c\text{-mod}}$ is midday modeled g_c, *Kr* is the mean root hydraulic conductance measured at each of the three soil water stress levels (Ψ_{soil} approximately −0.5, −1.5, and −2.5 MPa), $\Psi_{soil,md}$ is midday soil water potential that corresponds to the three Ψ_{soil}, $\Psi_{stem,md}$ is midday stem water potential estimated in transpiring plants at each $\Psi_{soil,md}$, VPD is leaf-to-air water vapor mole fraction difference and was fixed to 2 kPa (which is the average midday VPD measured in the glasshouse).

Statistical analysis

Differences between means were tested with Student's *t* tests after testing for normality and homogeneity of variances. We used linear regressions to quantify the correlation between pre-dawn tissue width variation and pre-dawn Ψ_{stem} in each plant individual used for *Kr* measurements. The relationship between g_c and Ψ_{soil} was determined by fitting a four-parameter sigmoid function of the form $y = y_0 + a/(1 + e^{(-(\Psi soil - x0)/b)})$ to the pooled midday g_c versus Ψ_{soil} data for both species. Results are presented as mean values ± SE. Differences were considered to be significant when $P < 0.05$. All analyses were performed using R version 3.5.3 (R Core Team, 2019). Figures were created using Sigmaplot version 12.5 (Systat Software Inc., San Jose, CA, USA).

Supplemental data

The following supplemental materials are available in the online version of this article.

Supplemental Figure S1. Stem water potential relaxation kinetics predicted using petiole and branchlet width displacement while rehydrating plants through the soil at different water stress levels.

Supplemental Figure S2. The set-up for *Kr* measurements in the woody *C. rhomboidea*.

Supplemental Figure S3. Simultaneous measurements of plant mass and stem water potential (Ψ_{stem}) in individual plants of *C. rhomboidea* and *T. cinerariifolium* to calculate the whole plant capacitance (C_{plant}).

Supplemental Figure S4. Rehydration kinetics of excised and intact petioles (attached to their leaf laminas) and branchlets in *T. cinerariifolium* and *C. rhomboidea*.

Supplemental Figure S5. Measured g_c and modeled $g_{c\text{-}mod}$ using observed *Kr*.

Acknowledgments

We thank Chris Lucani for technical support and Michelle Lang for glasshouse assistance.

Funding

This work was funded by the Tasmania Graduate Research Scholarship (Training Program Scholarship to I.B.), the Australian Research Council (LP170100103), and Botanical Resources Australia Pty Ltd.

Conflict of interest statement. There is no conflict of interest.

References

Andrews RE, Newman EI (1969) Resistance to water flow in soil and plant. New Phytol **68**: 1051–1058

Barrios-Masias FH, Knipfer T, McElrone AJ (2015) Differential responses of grapevine rootstocks to water stress are associated with adjustments in fine root hydraulic physiology and suberization. J Exp Bot **66**: 6069–6078

Blizzard WE, Boyer JS (1980) Comparative resistance of the soil and the plant to water transport 1. Plant Physiol **66**: 809–814

Bourbia I, Carins-Murphy MR, Gracie A, Brodribb TJ (2020) Xylem cavitation isolates leaky flowers during water stress in pyrethrum. New Phytol **227**: 146–155

Boyer JS, Kramer PJ (1995) Water Relations of Plants and Soils. Academic Press Inc, Cambridge, MA

Brodribb TJ, Bowman DJMS, Nichols S, Delzon S, Burlett R (2010) Xylem function and growth rate interact to determine recovery rates after exposure to extreme water deficit. New Phytol **188**: 533–542

Brodribb TJ, Cochard H (2009) Hydraulic failure defines the recovery and point of death in water-stressed conifers. Plant Physiol **149**: 575–584

Brodribb TJ, Holbrook NM (2003) Stomatal closure during leaf dehydration, correlation with other leaf physiological traits. Plant Physiol **132**: 2166–2173

Brodribb TJ, McAdam SAM (2013) Abscisic acid mediates a divergence in the drought response of two conifers1[W][OA]. Plant Physiol **162**: 1370–1377

Brodribb TJ, Powers J, Cochard H, Choat B (2020) Hanging by a thread? Forests and drought. Science **368**: 261–266

Brunner I, Herzog C, Dawes MA, Arend M, Sperisen C (2015) How tree roots respond to drought. Front Plant Sci **6**: 547

Carminati A, Javaux M (2020) Soil Rather Than Xylem Vulnerability Controls Stomatal Response to Drought. Trends Plant Sci **25**: 868–880

Carminati A (2013) Rhizosphere wettability decreases with root age: a problem or a strategy to increase water uptake of young roots? Front Plant Sci **4**: 298

Clarkson DT, Robards AW, Stephens JE, Stark M (1987) Suberin lamellae in the hypodermis of maize (Zea mays) roots; development and factors affecting the permeability of hypodermal layers. Plant Cell Environ **10**: 83–93

Correia MJ, Pereira JS (1995) The control of leaf conductance of white lupin by xylem ABA concentration decreases with the severity of water deficits. J Exp Bot **46**: 101–110

Cruz RT, Jordan WR, Drew MC (1992) Structural changes and associated reduction of hydraulic conductance in roots of Sorghum bicolor L. following exposure to water deficit. Plant Physiol **99**: 203–212

Cuneo IF, Barrios-Masias F, Knipfer T, Uretsky J, Reyes C, Lenain P, Brodersen CR, Walker MA, McElrone AJ (2020) Differences in grapevine rootstock sensitivity and recovery from drought are linked to fine root cortical lacunae and root tip function. New Phytol **229**: 272–283

Cuneo IF, Knipfer T, Brodersen CR, McElrone AJ (2016) Mechanical failure of fine root cortical cells initiates plant hydraulic decline during drought1[OPEN]. Plant Physiol **172**: 1669–1678

Cuneo IF, Knipfer T, Mandal P, Brodersen CR, McElrone AJ (2018) Water uptake can occur through woody portions of roots and facilitates localized embolism repair in grapevine. New Phytol **218**: 506–516

Domec JC, Scholz FG, Bucci SJ, Meinzer FC, Goldstein G, Villalobos-Vega R (2006) Diurnal and seasonal variation in root xylem embolism in neotropical savanna woody species: impact on stomatal control of plant water status. Plant Cell Environ **29**: 26–35

Dubrovsky JG, North GB, Nobel PS (1998) Root growth, developmental changes in the apex, and hydraulic conductivity for Opuntia ficus-indica during drought. New Phytol **138**: 75–82

Frensch J, Steudle E (1989) Axial and radial hydraulic resistance to roots of maize (Zea mays L.). Plant Physiol **91**: 719–726

Gambetta GA, Fei J, Rost TL, Knipfer T, Matthews MA, Shackel KA, Walker MA, McElrone AJ (2013) Water uptake along the length of grapevine fine roots: developmental anatomy, tissue-specific aquaporin expression, and pathways of water transport. Plant Physiol **163**: 1254–1265

Gardner WR, Ehlig CF (1962) Impedance to water movement in soil and plant. Science **138**: 522–523

Green SR, Clothier BE (1995) Root water uptake by kiwifruit vines following partial wetting of the root zone. Plant Soil **173**: 317–328

GulloM a. L, Nardini A, Salleo S, Tyree MT (1998) Changes in root hydraulic conductance (KR) of Olea oleaster seedlings following drought stress and irrigation. New Phytol **140**: 25–31

Hainsworth JM, Aylmore L a. G (1986) Water extraction by single plant roots. Soil Sci Soc Am J **50**: 841–848

Hallgren SW, Rüdinger M, Steudle E (1995) Root hydraulic properties of spruce measured with the pressure probe. *In* F Baluška, M Čiamporová, O Gašparíková, PW Barlow, eds, Structure and Function of Roots: Proceedings of the Fourth International Symposium on Structure and Function of Roots, June 20–26, 1993, Stará Lesná, Slovakia. Springer, Dordrecht, Netherlands, pp 215–222

Hansen GK (1974) Resistance to water transport in soil and young wheat plants. Acta Agric Scand **24**: 37–48

Holloway-Phillips M-M, Brodribb TJ (2011) Minimum hydraulic safety leads to maximum water-use efficiency in a forage grass. Plant Cell Environ **34**: 302–313

Jarvis PG, McNaughton KG (1986) Stomatal control of transpiration: scaling up from leaf to region. *In* A MacFadyen, ED Ford, eds, Advances in Ecological Research. Cambridge, MA: Academic Press, pp 1–49

Korson L, Drost-Hansen W, Millero FJ (1969) Viscosity of water at various temperatures. J Phys Chem **73**: 34–39

Kramer PJ (1950) Effects of wilting on the subsequent intake of water by plants. Am J Bot **37**: 280–284

Kramer PJ, Bullock HC (1966) Seasonal variations in the proportions of suberized and unsuberized roots of trees in relation to the absorption of water. Am J Bot **53**: 200–204

Liang J, Zhang J (1999) The relations of stomatal closure and reopening to xylem ABA concentration and leaf water potential during soil drying and rewatering. Plant Growth Regul **29**: 77–86

Liang J, Zhang J, Wong MH (1997) Can stomatal closure caused by xylem ABA explain the inhibition of leaf photosynthesis under soil drying? Photosynth Res **51**: 149–159

Loewenstein NJ, Pallardy SG (2002) Influence of a drying cycle on post-drought xylem sap abscisic acid and stomatal responses in young temperate deciduous angiosperms. New Phytol **156**: 351–361

Ma Z, Guo D, Xu X, Lu M, Bardgett RD, Eissenstat DM, McCormack ML, Hedin LO (2018) Evolutionary history resolves global organization of root functional traits. Nature **555**: 94–97

Martre P, North GB, Nobel PS (2001) Hydraulic conductance and mercury-sensitive water transport for roots of Opuntia acanthocarpa in relation to soil drying and rewetting. Plant Physiol **126**: 352–362

Maurel C, Boursiac Y, Luu D-T, Santoni V, Shahzad Z, Verdoucq L (2015) Aquaporins in plants. Physiol Rev **95**: 1321–1358

Newman EI (1969) Resistance to water flow in soil and plant. I. Soil resistance in relation to amounts of root: theoretical estimates. J Appl Ecol **6**: 1–12

Nobel PS, Cui M (1992) Hydraulic conductances of the soil, the root-soil air gap, and the root: changes for desert succulents in drying soil. J Exp Bot **43**: 319–326

Nobel PS, Sanderson J (1984) Rectifier-like activities of roots of two desert succulents. J Exp Bot **35**: 727–737

North G, Nobel P (1991) Changes in hydraulic conductivity and anatomy caused by drying and rewetting roots of Agave deserti (Agavaceae). Am J Bot **78**: 906

North GB, Martre P, Nobel PS (2004) Aquaporins account for variations in hydraulic conductance for metabolically active root regions of Agave deserti in wet, dry, and rewetted soil. Plant Cell Environ **27**: 219–228

North GB, Nobel PS (1992) Drought-induced changes in hydraulic conductivity and structure in roots of Ferocactus acanthodes and Opuntia ficus-indica. New Phytol **120**: 9–19

North GB, Nobel PS (1996) Radial hydraulic conductivity of individual root tissues of Opuntia ficus-indica (L.) miller as soil moisture caries. Ann Bot **77**: 133–142

Otsu N (1979) A threshold selection method from gray-level histograms. IEEE Trans Syst Man Cybernet **9**: 62–66

Passioura J (1980) The transport of water from soil to shoot in wheat seedlings. J Exp Bot **31**: 333–345 doi: 10.1093/jxb/31.1.333

Passioura JB (1988) Water transport in and to roots. Ann Rev Plant Physiol Plant Mol Biol **39**: 245–265

Pou A, Flexas J, del Alsina M M, Bota J, Carambula C, Herralde FD, Galmés J, Lovisolo C, Jiménez M, Ribas-Carbó M, et al. (2008) Adjustments of water use efficiency by stomatal regulation during drought and recovery in the drought-adapted Vitis hybrid Richter-110 (V. berlandieri × V. rupestris). Physiol Plant **134**: 313–323

Rehschuh R, Cecilia A, Zuber M, Faragó T, Baumbach T, Hartmann H, Jansen S, Mayr S, Ruehr N (2020) Drought-induced xylem embolism limits the recovery of leaf gas exchange in scots pine. Plant Physiol **184**: 852–864

Rodriguez-Dominguez CM, Brodribb TJ (2019) Declining root water transport drives stomatal closure in olive under moderate water stress. New Phytol **225**: 126–134

Rossatto DR, Silva LCR, Sternberg LSL, Franco AC (2014) Do woody and herbaceous species compete for soil water across topographic gradients? Evidence for niche partitioning in a Neotropical savanna. South African J Bot **91**: 14–18

Ruehr NK, Grote R, Mayr S, Arneth A (2019) Beyond the extreme: recovery of carbon and water relations in woody plants following heat and drought stress. Tree Physiol **39**: 1285–1299

Schenk HJ, Jackson RB (2002) Rooting depths, lateral root spreads and below-ground/above-ground allometries of plants in water-limited ecosystems. J Ecol **90**: 480–494

Scholz FG, Phillips NG, Bucci SJ, Meinzer FC, Goldstein G (2011) Hydraulic capacitance: biophysics and functional significance of internal water sources in relation to tree size. *In* FC Meinzer, B Lachenbruch, TE Dawson, eds, Size- and Age-Related Changes in Tree Structure and Function. Springer, Dordrecht, Netherlands, pp 341–361

Scoffoni C, Albuquerque C, Cochard H, Buckley TN, Fletcher LR, Caringella MA, Bartlett M, Brodersen CR, Jansen S, McElrone AJ, et al. (2018) The causes of leaf hydraulic vulnerability and its influence on gas exchange in Arabidopsis thaliana. Plant Physiol **178**: 1584–1601

Scoffoni C, McKown AD, Rawls M, Sack L (2012) Dynamics of leaf hydraulic conductance with water status: quantification and analysis of species differences under steady state. J Exp Bot **63**: 643–658

Torres-Ruiz JM, Díaz-Espejo A, Perez-Martin A, Hernandez-Santana V (2015) Role of hydraulic and chemical signals in leaves, stems and roots in the stomatal behaviour of olive trees under water stress and recovery conditions. Tree Physiol **35**: 415–424

Trifilò P, Raimondo F, Nardini A, Lo Gullo MA, Salleo S (2004) Drought resistance of Ailanthus altissima: root hydraulics and water relations. Tree Physiol **24**: 107–114

Tsuda M, Tyree MT (2000) Plant hydraulic conductance measured by the high pressure flow meter in crop plants. J Exp Bot **51**: 823–828

Tyree MT, Patiño S, Bennink J, Alexander J (1995) Dynamic measurements of roots hydraulic conductance using a high-pressure flowmeter in the laboratory and field. J Exp Bot **46**: 83–94

Tyree MT, Zimmermann MH (2002) Xylem Structure and the Ascent of Sap, 2nd ed. Springer-Verlag, Berlin Heidelberg

Vandeleur RK, Mayo G, Shelden MC, Gilliham M, Kaiser BN, Tyerman SD (2009) The role of plasma membrane intrinsic protein aquaporins in water transport through roots: diurnal and drought stress responses reveal different strategies between isohydric and anisohydric cultivars of grapevine. Plant Physiol **149**: 445–460

Wang X, Du T, Huang J, Peng S, Xiong D (2018) Leaf hydraulic vulnerability triggers the decline in stomatal and mesophyll conductance during drought in rice. J Exp Bot **69**: 4033–4045

Yan W, Zheng S, Zhong Y, Shangguan Z (2017) Contrasting dynamics of leaf potential and gas exchange during progressive drought cycles and recovery in Amorpha fruticosa and Robinia pseudoacacia. Sci Rep **7**: 4470

Zhang YJ, Rockwell FE, Graham AC, Alexander T, Holbrook NM (2016) Reversible leaf xylem collapse: a potential "circuit breaker" against cavitation. Plant Physiol **172**: 2261–2274